Chem Soc Rev

Aromaticity in Transition Structures

Journal:	*Chemical Society Reviews*
Manuscript ID:	CS-REV-01-2014-000012.R1
Article Type:	Tutorial Review
Date Submitted by the Author:	19-Feb-2014
Complete List of Authors:	von Rague Schleyer, Paul; Computational Chemistry Annex, The University of Georgia Wu, Judy I-Chia; University of Georgia, Cossio, Fernando; University of the Basque Country, Organic Chemistry I Fernandez, Israel; Universidad Complutense de Madrid, Organic Chemistry I

This Tutorial Review will present briefly the interpretative tools provided by computational chemistry to describe and quantify the different manifestations of aromaticity in transition structures.
240x142mm (72 x 72 DPI)

Aromaticity in Transition Structures

Paul von Ragué Schleyer,[a] Judy I. Wu,[a] Fernando P. Cossío*[b] and Israel Fernández*[c]

[a]Department of Chemistry, Center for Computational Chemistry, University of Georgia, Athens, Georgia 30602, United States.
[b]Departamento de Química Orgánica I-Kimika Organikoa I Saila, Facultad de Química-Kimika Fakultatea, Universidad del País Vasco–Euskal Herriko Unibertsitatea, and Donostia International Physics Center (DIPC), P. K. 1072, 20080 San Sebastián-Donostia (Spain). E-mail: fp.cossio@ehu.es
[c]Departamento de Química Orgánica I, Facultad de Ciencias Químicas, Universidad Complutense de Madrid, 28040, Madrid, Spain. Fax: +34-3944310. E-mail: israel@quim.ucm.es.

Abstract

Aromaticity is an essential concept in chemistry, employed to account for the unusual stability, reactivity, molecular structures, and other properties of many unsaturated organic compounds. This concept was later extended to inorganic molecules and to saturated systems with mobile electrons, as well as to transition structures, the focus of the present review. Although transition structures are inherently delocalized, not all exhibit aromaticity. We contrast here examples of pericyclic reaction transition structures (where aromaticity is significant) with those for illustrative pseudo-pericyclic reactions (where aromaticity is less or not important). Non-pericylic reactions also may have aromatic transition structures. State-of-the-art computational methods to evaluate the aromaticity of transition structures are described briefly.

Key learning points:

(1) Quantifying aromaticity in transition structures
(2) Various types of aromaticity in pericyclic transition structures
(3) Distinction between pericyclic and pseudopericyclic reactions
(4) Aromaticity in non-pericyclic transformations

1. Introduction.

Evans and Warhurst's recognition in 1938[1] of the relationship between the six π electrons of benzene and the six delocalized electrons in the cyclic transition structure of the Diels-Alder (DA) reaction between butadiene and ethylene was the seminal insight leading to the rationalization and current understanding of the aromatic character exhibited by transition states. Note that the DA transition structure envisioned in 1938 surely did not meet the commonly enunciated aromaticity criteria (planar, bond length-equalized rings having clear-cut π character). Moreover, the aromaticity concept itself is fraught with ambiguities. Indeed, it has been described as a "typical example of an unicorn of chemical bonding models," because of its virtual, rather than experimentally observable, nature.[2] The application of this idea to transition structures has contributed enormously to our current understanding of molecular reactivity.[3] As Evans pointed out in 1939, *"the greater the mobility of the π electrons in the transition state, the greater will be the lowering of the activation energy."*[4] The relationship between aromaticity in transition structures and chemical reactivity was later generalized based on symmetry considerations through the Woodward-Hoffman rules[5] and the Zimmerman-Dewar Hückel-Möbius concept.[6] Although initially applied only to pericyclic reactions, aromaticity in transition states was also extended to characterize and interpret the reaction rates and outcomes of pseudo-pericyclic and non-pericyclic reactions.

Given the difficulties associated with the experimental quantification of aromaticity, Computational Chemistry emerges as an essential tool to probe the aromatic character of a compound. This Tutorial Review will present briefly the interpretative tools provided by computational chemistry to describe and quantify the different manifestations of aromaticity in transition structures. The influence of the different types of aromaticity on reactivity is illustrated by presenting selected representative examples of different types of transformations ranging from pericyclic to non-pericyclic processes.

2. Quantitative Evaluations of Aromaticity in Transition Structures

This section briefly describes currently used computational methods (and their limitations) to evaluate transition state aromaticity. Because of the elusive character of transition structures, computational chemistry has become the key means of identifying, understanding, interpreting, and quantifying their aromaticity. As transition structures (TSs) are inherently more delocalized than local minima, TSs tend to display enhanced aromatic properties, including bond length equalization, special magnetic responses (associated with induced ring currents), and unusually large energetic stabilizations (resonance energies).[7] The growing sophistication and versatility of *ab inito* and density functional theory (DFT) computations, which can be employed more effectively than experimental approaches, aids the investigation of geometric, magnetic, and energetic aromaticity in transition structures.

2.1. Structural and Energetic Criteria for Transition Structure Aromaticity

Since energetic properties largely govern the chemical behaviour of molecules (e.g., their reactivity), enhanced thermochemical stability is a key indicator for transition structure aromaticity.

But how can the energetic consequences of aromaticity in transition structures be measured? Like evaluations of the aromatic stabilization energies of aromatic molecules, which depend on selecting appropriate non-aromatic comparison references,[8] estimates of the aromatic stabilization energies of aromatic transition structures also are based on *relative* comparisons. For example, the minima of ground state aromatic molecules (e.g., benzene) have π resonance stabilization energies lower "than they ought to be" (i.e., when compared to appropriate non-aromatic references such as three butadiene conjugations). Likewise, aromatic transition structures often feature a large *energy of concert* (E_c).[9] The E_c of a pericyclic reaction is estimated as the difference between the measured activation energy for

the actual (concerted) process deduced by using empirical "group increments" and the estimated barrier for an alternative stepwise hypothetical diradical pathway.

"The anthracene problem"[10] illustrates the inadequacy of reactivity as an aromaticity criterion. Despite the greater aromaticity of the anthracene central ring (based on geometric and magnetic considerations),[10] it is more prone towards DA cycloaddition than the less aromatic outer rings. This anomaly, which refutes the (erroneous) textbook characterization of aromatic molecules, as being not only more *thermochemical stable than they ought to be* but also kinetically *less reactive than they ought to be*, has been (and still is) under much debate.[11] A simple explanation is that the transition structure for cycloaddition to the central ring is stabilized more aromatically due to the incipient formation of a second (additional) aromatic Clar ring in the product. Conversely, cycloaddition through the less aromatic side rings proceeds through a higher energy transition structure, where no such *extra* aromatic Clar stabilization is present. Thus, the greater effect of aromaticity on the relative transition structure energies (rather than on the ground state aromaticity of the central vs. side rings) dictates the activation barriers and reactivity of anthracene.

Geometrically, bond length equalization is the most direct structural indicator for aromaticity. Many structure-based aromaticity indices are based on reference values for standard aromatic molecules.[12] However, such procedures cannot be implemented easily for transition structures, and other approaches are required. For instance, the synchronicity (*Sy*) index, which quantifies the degree of structural transformation of the forming/breaking *n* bonds from the reactants (R) to the products (P) via the cyclic transition structure (TS), can be defined as:

$$Sy = 1 - (2n-2)^{-1} \sum_{i=1}^{n} \frac{|\delta B_i - \delta B_{av}|}{\delta B_{av}}$$

where δB_i represents the relative variation of a given bond index at the TS with respect to those of the reactants and products following the expression:

$$\delta B_i = \frac{\delta B_i^{TS} - \delta B_i^R}{\delta B_i^P - \delta B_i^R}$$

and δB_{av} is simply the average value of δB_i:

$$\delta B_{av} = n^{-1} \sum_{i=1}^{n} \delta B_i$$

Based on this definition, aromatic transition structures that are subject to enhanced electron delocalization display high synchronicity ($Sy \approx 1$), i. e., when $\delta B_i \approx \delta B_{av}$ for the bonds being formed and broken along a cyclic array. This analysis has been confirmed in 1,3-dipolar cycloadditions.[13] However, high synchronicity is NOT a sufficient condition for an aromatic transition structure; additional, less ambiguous criteria are required as well. For example, Sakai's Index of Deviation from Aromaticity (IDA) method,[14] which considers both bond length equalization and the resonance stabilization energy associated with transition structures, performs reasonably well for pericyclic reactions.

2.2. Magnetic Descriptors: Ring Currents, Magnetic Susceptibility Exaltations, Nucleus Independent Chemical Shifts

Cyclically delocalized π and σ electrons that participate in the bond forming and bond breaking processes of pericyclic reactions lead to induced ring currents; these result in distinct magnetic properties for aromatic transition structures and serve as the basis for quantifying magnetic aromaticity. Pauling's ring current theory (1936) first envisioned that the p_z electrons of cyclic π conjugated aromatic ring carbon atoms might circulate freely in the presence of external applied magnetic field.[15] This assumption was elaborated by London (1937) in terms of quantum theory.[16] This pioneering work as well as the advent of NMR spectroscopy led to Pople's (1956) ring current model, which explained the anomalous

behaviour of arene ^{1}H NMR chemical shifts.[17] The ability to sustain an induced diatropic ring current, either in two or three dimensions, also is a hallmark of transition state aromaticity.

In practice, magnetic-based evaluations of transition state aromaticity are less arbitrary than structural and energetic-based criteria. Magnetic aromaticity can be evaluated by computing magnetic responses arising from the induced ring currents or by probing the ring current directly. Aromatic molecules have characteristic ^{1}H NMR chemical shifts, diamagnetic susceptibility exaltations (Λ), and magnetic susceptibility anisotropies. However, these criteria have their limitations, e.g., ^{1}H nuclei are needed and appropriate references for evaluating magnetic susceptibility exaltations may be difficult to select and justify.

The challenge of quantifying magnetic aromaticity is the difficulty in identifying magnetic responses associated exclusively with aromaticity, since lone pairs, atom cores, and irrelevant σ-electrons (i.e., those not related to the principal induced "π" or aromatic ring current), also respond to external applied magnetic fields. ^{1}H NMR chemical shifts, for instance, include blends of "local" magnetic effects not related to aromaticity. Unlike energetic evaluations of aromaticity (e.g., based on resonance energies or aromatic stabilization energies), which reflect a global property of the whole molecule, the magnetic responses of aromatic molecules can be probed both *globally* (e.g., exalted diamagnetic susceptibilities and anisotropies for the entire molecule) and more *locally* (e.g., NICS at specific reference points in and near molecules, see below). As their size-dependency may differ appreciably, global and local magnetic aromaticity evaluations may lead to apparently conflicting conclusions.

Magnetic susceptibility (χ) is the degree of magnetization that arises from a compound in response to an applied magnetic field. Aromatic compounds display enhanced diamagnetic susceptibilities as their induced magnetic fields oppose the externally applied magnetic field. Dauben's 1968 generalization of the use of diamagnetic susceptibility exaltations (Λ^m) as a

measure for aromaticity defined Λ^m as the increase in magnetic susceptibility of an aromatic molecule (A) compared to the molar susceptibility sums of its bond increments, usually based on the magnetic susceptibilities of delocalized non-aromatic reference compounds ($\Lambda^m = \chi_A - \chi_{ref}$). [18] Thus, compounds with $\Lambda^m > 0$ are aromatic and have exalted diamagnetic susceptibilities whereas those with $\Lambda^m < 0$ are antiaromatic and should display exalted paramagnetic susceptibilities. Non-aromatic species have Λ^m values close to zero. The main criticisms of diamagnetic susceptibility exaltation criteria are two-fold: (i) magnetic susceptibilities depend on the square of the ring area, and (ii) magnetic susceptibility exaltations depend on the reference compounds selected for comparison. Local magnetic probes of aromaticity, like ^{1}H NMR chemical shifts and NICS (see below), do not have these problems (although they are not free from other complications).

Nucleus Independent Chemical Shift (NICS)[7, 19] computations in their most sophisticated modern refinements are highly advantageous for quantifying magnetic aromaticity in transition structures, as such evaluations do not rely on reference compounds, are easy to compute, and have been refined to isolate magnetic effects related to aromaticity exclusively (i.e., dissected molecular orbital-based MO-NICS$_{zz}$).[20] NICS values at selected positions, or grids of such points probe the chemical shielding effects in the vicinity of the molecules; for example, NICS(0) designates the isotropic value at the heavy atom centre of the reacting bonds. Ring (or cage) critical points as defined within Quantum Theory of Atoms in Molecules (QTAIM) may be used for NICS as well. Aromatic/Antiaromatic molecules have characteristic negative (diamagnetic)/positive (paramagnetic) NICS values in the ring and positive/negative NICS values outside of the ring as a result of their diatropic/paratropic ring currents. The signs of the computed NICS values are reversed to conform to the experimental upfield (negative) and downfield (positive) NMR chemical shifts convention.

Rather than the original isotropic Nucleus Independent Chemical Shift values (e.g., NICS(0) and NICS(1), (i.e., at 1 Å above a ring center), the hierarchy of refined NICS indices[20] eliminate magnetic responses not related to aromaticity and exemplify the usefulness of this method best. Thus, the "*zz*" vector component of isotropic NICS (i.e., $NICS_{zz}$, the response perpendicular to the "ring" of cyclically delocalized electrons) reflects "aromaticity" better than isotropic NICS values (which are contaminated by irrelevant "*xx*" and "*yy*" vector components). Several computational programs, e.g., deMon-NMR, MAG-ReSpect, ADF, and NBO, afford effective implementations of $NICS_{zz}$ and its subsequent dissection into individual LMO (localized molecular orbital) or CMO (canonical molecular orbital) contributions.[20,21] LMO-NICS based on the IGLO (individual gauge for localized orbital) method evaluates the computed shielding tensor in terms of individual localized molecular orbitals and assigns a separate gauge origin for each localized molecular orbital. For pericyclic transition structures, which usually adopt non-planar geometries, this method is limited by the difficulty of achieving unambiguous σ and π orbital separation when various localization algorithms, e.g., the Pipek-Mezey, Foster-Boys, or Bohman-Weinhold (NBO) localization, are applied to obtain a unitary transformed set of localized molecular orbitals equivalent to the corresponding CMO's. CMO-NICS, computed by the GIAO (gauge-independent atomic orbital) method, evaluates the shielding tensor of each canonical molecular orbital with individual gauge origins for each atomic orbital and avoids such difficulties. Dissected LMO- and CMO-NICS provide complementary insights for evaluating the aromaticity of minima and transition structures.

Visual descriptions of the induced ring current density, e.g., based on computed GIMIC[22] (Gauge-Including Magnetically Induced Current) and ACID,[23] (Anisotropy of the Current-Induced Density) plots, also provide insightful "maps" for understanding transition state aromaticity.

3. Representative Examples

3.1 Pericyclic Reactions

As noted above, the concept initially proposed by Evans and Warhurst[1] has been applied extensively to thermally allowed pericyclic reactions.[3] This section presents a selection of pericyclic transformations (defined as reactions in which concerted reorganization of bonding takes place throughout a cyclic array of continuously bonded atoms), which represent and illustrate the different types of aromaticity exhibited by transition structures.

3.1.1. 4*n*+2 pericyclic reactions

Both benzene and the Diels-Alder transition structure of butadiene and ethylene are stabilized by resonance (electron delocalization of 4*n*+2 numbers of electrons in a closed circuit) and display towards CC bond length equalization tendencies. This analogy applies to the aromatic transition structures of thermally allowed pericyclic reactions involving 4*n*+2 electrons (Figure 1). Hence, cycloaddition and electrocyclic reactions often favour mechanistic routes involving aromatic transition structures due to the lower activation barriers. As electron delocalization effects arise from orbital interactions, the enhanced electron mobility facilitated in the aromatic transition structures of pericyclic reactions also lead to more bond length-equalized geometries and follow more synchronized reaction paths.

For example, the Diels-Alder cycloaddition of butadiene and ethylene (Figure 1b) favours a concerted reaction through a six delocalized-electron transition structure over the alternative stepwise diradical mechanism by 2-7 kcal/mol.[24,25] This is documented by the large negative NICS value computed at the centre of the ring being formed in **TS1** (NICS(0) = –19.4 ppm, Figure 1b). The trimerization of acetylene **4** to benzene **1** (Figure 1c) proceeds via an aromatic D_{3h} transition structure **TS2** and can be compared with benzene directly (see below). The electrocyclization of 1,3,5-hexatriene **5** to 1,3-cyclohexadiene **6** (Figure 1d) also

favours a concerted reaction pathway (activation barrier: 29 kcal/mol), through an aromatic transition structure **TS3** (NICS(0) = –14.3 ppm),[24] over the alternative stepwise diradical route (activation barrier: 42-45 kcal/mol). The degenerate [3,3] Cope rearrangement of 1,5-hexadiene **7** (Figure 1e)[26] is concerted and proceeds via an aromatic chair-like transition structure analogous to **TS4** (NICS(0) = –23.3 ppm).

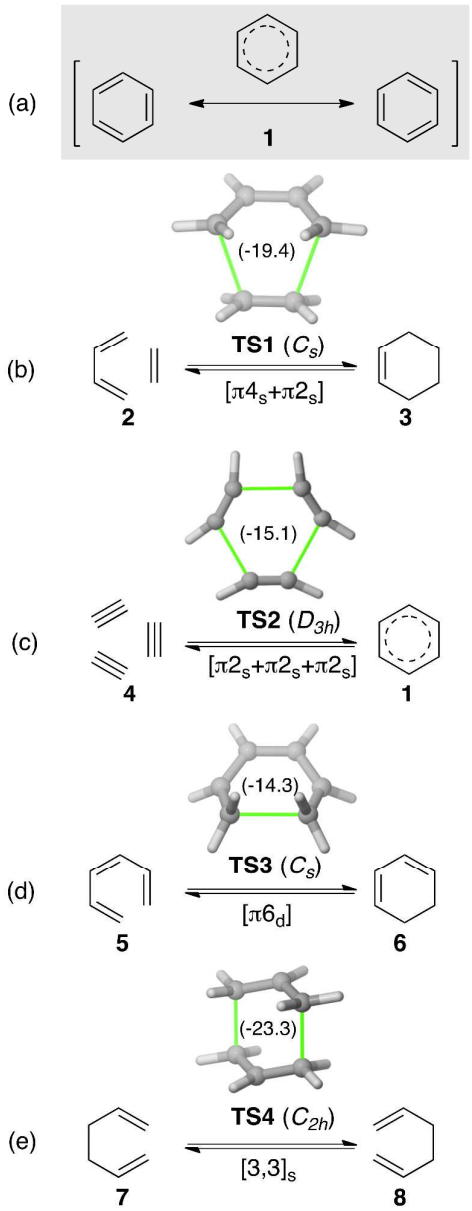

Figure 1. Archetypal examples of symmetry allowed thermal pericyclic reactions (b)-(e) involving six electrons. The analogy between **TS1-TS4** and benzene **1** (a) is emphasized. NICS(0) values (given in ppm, in parentheses) were computed at the heavy atom centres of the cycles.

Like benzene, these transition structures (**TS1-TS4**) involve the delocalization of six electrons, but the participation of σ orbitals and in-plane π orbitals promote very different aromaticity behaviour. For example, the computed NICS grids (NICS points placed along an axis *z* perpendicular to the molecular plane) plotted for the aromatic **TS2** (six *in-plane* π electrons) and benzene **1** (six *out-of-plane* π electrons) are drastically different (Figure 2). Thus, in **TS2** there is a monotonous decay of the NICS values on going from the molecular plane to larger values of *z*, whereas in **1** the maximum negative NICS is reached at a certain distance $z = R_0$ above or below the molecular plane. Hence, transition structures like **TS2** exhibit *in-plane* aromaticity with a diamagnetic ring current σ_{zz}^{d} and are described as:[27]

$$\sigma_{zz}^{d} = AR_{av}^{-1}\left[1+\omega^2\right]^{-3/2}$$

where A is a constant and $\omega = R_{av}^{-1}\left(z-a\right)$, with $a = 0$, as the diatropic electron circulation takes place in the molecular plane, and the maximum diamagnetic shielding occurs therefore at $\omega = 0$. In benzene, there are two diatropic ring currents circulating at $a = \pm R_0$, thus, the maximum shielding for which $\omega = 0$ is reached when $z = \pm R_0$. This simple model connects the physical interpretation of the behaviour of the NICS with Pauling, London, and Pople's ring current models.[15-17] A similar behaviour has been observed for 1,3-dipolar reactions,[13] but no direct correlation between aromaticity and regioselectivity could be established for model (3+2) cycloadditions between nitrones and alkenes.

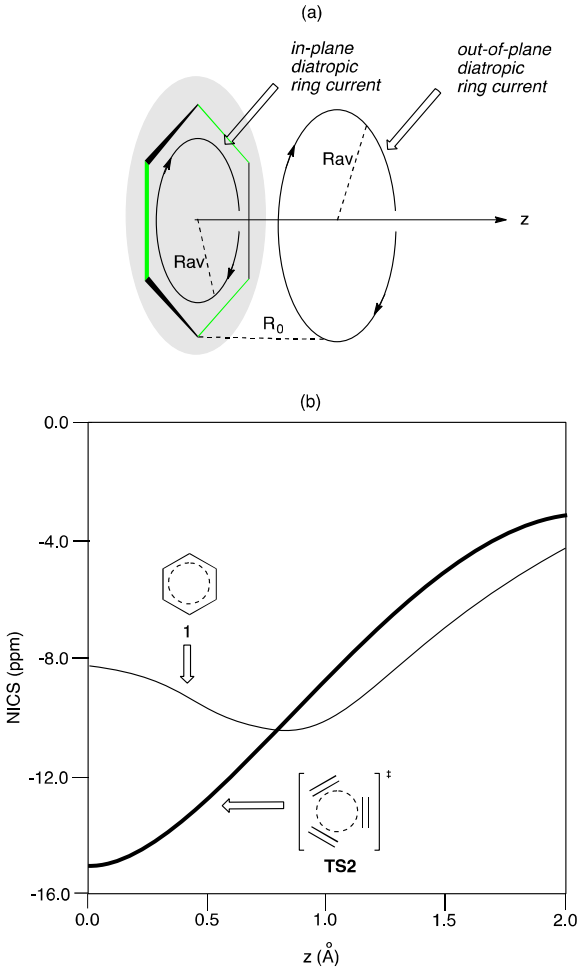

Figure 2. (a) Schematic representation of the diatropic ring currents in transition structure **TS2** and benzene **1**. (b) NICS vs. *z* c for both **TS2** and **1**.

Notably, thermally allowed, strongly exothermic reactions, involving aromatic transition structures also can have high *absolute* activation barriers. For example, the trimerization of acetylene **4** to benzene **1** (see Figure 1c) is highly exothermic (–143 kcal/mol), but the computed activation barrier via **TS2** is extremely high (+80 kcal/mol)![28] Just as aromatic molecules can be thermochemically stabilized by aromaticity but destabilized by other structural features simultaneously, activation barriers involving aromatic transition states also can be raised as a consequence of other electronic and geometric factors. The high activation barrier for the trimerization of acetylene arises from both the energy required to geometrically distort three ethylenes from their linear geometries as well as closed shell

repulsion between the filled in-plane π orbitals. Within conceptual Valence Bond theory,[29] this large activation energy can be rationalised in terms of the considerable adiabatic singlet-triplet gap for the (2+2+2) reaction as compared with that of 1,3-butadiene + ethylene reacting system.

Regarding the commonly imposed relationships among thermochemical stability, aromaticity, and reactivity, we emphasize that reactivity, which depends on the relative energies of the product and transition state of a reaction, is *not* a valid criterion for aromaticity. Thus, note Evans and Warhurst's comment, *"conjugated molecules show on the one hand enhanced thermochemical stability, while on the other hand they show in some of their reactions greater reactivity than do non-conjugated substances."*[1] Indeed, reactions proceeding through aromatic transition states have lower activation barriers and display faster rates, but the purported "aromatic stabilization" is established based on comparisons to the transition states of alternative stepwise reaction routes. Likewise, the aromaticities of ground state minimum molecules should be based on comparisons to other ground state minimum reference molecules. In the parent butadiene + ethylene DA reaction, only the transition structure is aromatic (the reactant and products are all non-aromatic), and as a consequence, the activation barrier is lowered and a fast reaction rate is anticipated. Remarkably, Jiao and Schleyer observed appreciable catalytic electrostatic accelerations for electrocyclic reactions by metal cation complexation, as metal complexation led to a much greater electrostatic stabilization for the transition structures than for the ground states of 1,3,-*cis*-5-hexatriene and 1,3-cyclohexadiene cyclizations, the 1,5-H shifts of cyclopentadiene and penta-1,3-diene, as well as the Cope rearrangement of semibuvallene.[3]

High order pericyclic reactions involving $4n+2$ electrons, for which $n \geq 2$, have been scarcely studied. In these cases, the problem of periselectivity, namely the selectivity between different symmetry allowed processes, emerges as an additional feature.[30] McIver[31] suggested

that the concertedness of cycloaddition reactions should diminish with increasing ring size of the corresponding transition structures. Rzepa and Wylie[32] analysed the mechanism of different cycloadditions as a function of ring size and concluded that the crossover for high order pericyclic reactions probably occurs for transition structures involving ten-membered cyclic structures. More recently, Alder et al.[33] have predicted that [$\pi 6_s + \pi 4_s$] cycloadditions can take place in a concerted manner with a proper choice of substituents. In terms of periselectivity, the major obstacle to overcome arises from the competitive [$\pi 4_s + \pi 2_s$] and Cope rearrangements. In [8+2] cycloadditions there are also 6-electron competitive pericyclic processes and in many cases the cycloaddition, if it occurs, is stepwise.[34] Concerted but highly asynchronous [$\pi 8_s + \pi 2_s$] reaction can take place with highly pre-organised substrates such as benzynes and imidazo[1,2-a]pyridines or the corresponding pyrimidine analogues.[34]

3.1.2. Pericyclic Reactions Involving Möbius Transition Structures

We describe the *Möbius aromaticity* concept briefly before discussing details of reactions involving Möbius transition structures.[35]

In 1964, Heilbronner noted that there was no loss of π-electron resonance energy in closed-shell systems with [4*n*] π-electrons distributed along a Möbius strip having a single half twist (Figure 3).[36] His seminal paper focused on different conformations of annulenes to describe how idealized π orbitals can be twisted to form a Möbius strip showing, in addition, that molecules with [4*n*] π electrons in their peripheries can be stabilized without introducing any apparent bond-angle or steric repulsion strains when the number of carbon atoms in the annulene is larger than ~20. In sharp contrast to the Hückel-rule, those systems with [4*n*+2] π electrons would be destabilized. Thus, annulenes with non-planar equilibrium geometries

containing [4*n*] π-electrons (with n > 5) in their peripheries are considered as 'Möbius aromatic', whereas those possessing [4*n*+2] π-electrons are 'Möbius antiaromatic'.

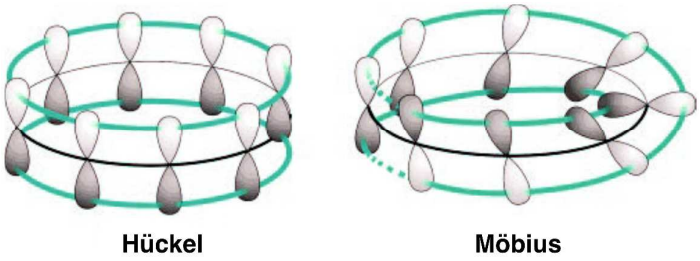

Figure 3. A Hückel annulene and idealized equilateral Möbius annulene (Figure adapted from R. Herges, *Chem. Rev.* 2006, **106**, 4280).

Möbius aromaticity is most effectively identified based on considerations of magnetic susceptibility exaltations and computed large negative NICS values.[3] On this basis, Schleyer and co-workers characterized the first Möbius aromatic molecule, $(CH)_9^+$ **8** (see Figure 4),[37] which displayed notable bond length equalization, exalted diamagnetic susceptibility, and a negative isotropic NICS value, satisfying the structural and magnetic criteria for aromaticity. Nevertheless, the synthesis and characterization of novel systems exhibiting Möbius aromaticity remains a challenging goal.

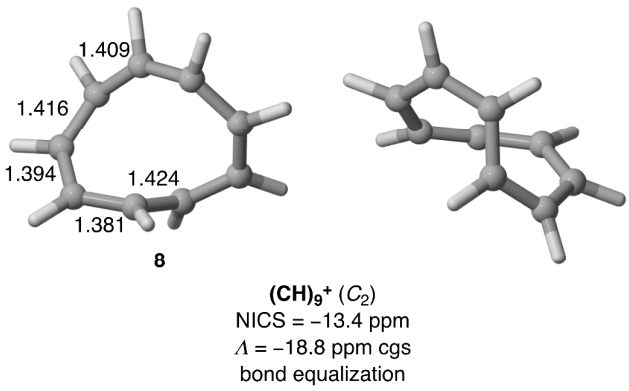

Figure 4. The first reported computed example of a Möbius-aromatic molecule, $(CH)_9^+$. Geometry taken from reference 37. Bond lengths are given in Å.

Zimmerman incorporated the Möbius concept into his reformulation of the original Woodward–Hoffmann selection rules for pericyclic reactions.[6] Thus, the preferred outcome of a pericyclic reaction can be predicted by analysing whether the transition structure might exhibit Huckel or Möbius aromaticity. On this basis, a transition structure with a local C_s symmetry plane and $4n+2$ mobile electrons would have Hückel rather than Möbius aromaticity.

Various pericyclic transformations proceed through Möbius aromatic transition structures. Among them, we have selected three representative cases: (i) the [1,7]-sigmatropic migration of a hydrogen atom in (*Z,Z*)-1,3,5-heptatriene[35a] (Figure 5a) (ii) the isomerization of (*Z,E,Z,E,Z,E*)-[12]annulene (the most stable $(CH)_{12}$ isomer) to (*Z,Z,Z,E,Z,E*)-[12]annulene[35a] (Figure 5b), and (iii) the electrocyclisation of *Z,E,Z*-decapentaene[38] (Figure 5c). In (i), the transition structure for **9** $\rightarrow$ **10** adopts a half-twist Möbius topology (Figure 5a), displays notable bond length equalization (C–C bond distances in the range of 1.35 to 1.41 Å), and the sp^2 hybridised "ring" protons exhibit downfield ^{1}H-NMR chemical shifts (δ = 6.3-6.9 ppm) comparable to those of benzene. Likewise, the Möbius aromatic transition structure for **11** $\rightarrow$ **12** in (ii) (Figure 5b) displays C–C bond length equalization (1.38 to 1.41 Å range), a large negative isotropic NICS value (–13.9 ppm), and exalted diamagnetic susceptibility (Λ = –43.8 cgs ppm). Importantly, this transformation clearly illustrates that Möbius aromatic transition structures (i.e. having the Möbius strip topology) do not necessarily involve forming or breaking bonds, but coupled valence shifts and bond rotations also can evoke Möbius aromaticity. In (iii), the 10 electron ($4n+2$) electrocyclisation of *Z,E,Z*-decapentaene **13** occurs through a transition structure that possesses a *double-twist* Möbius strip topology to form **14** (Figure 5c). The aromatic nature of **TS7** is confirmed by its equalized C–C bond lengths and computed large negative NICS(0) (–14.9 ppm) value.[38] The latter exemplifies Rzepa's statement nicely,[38] "*pericyclic reactions via double-twist Möbius aromatic conformation*

could formally be regarded as an extension to the selection rules originally formulated by Zimmerman".[6]

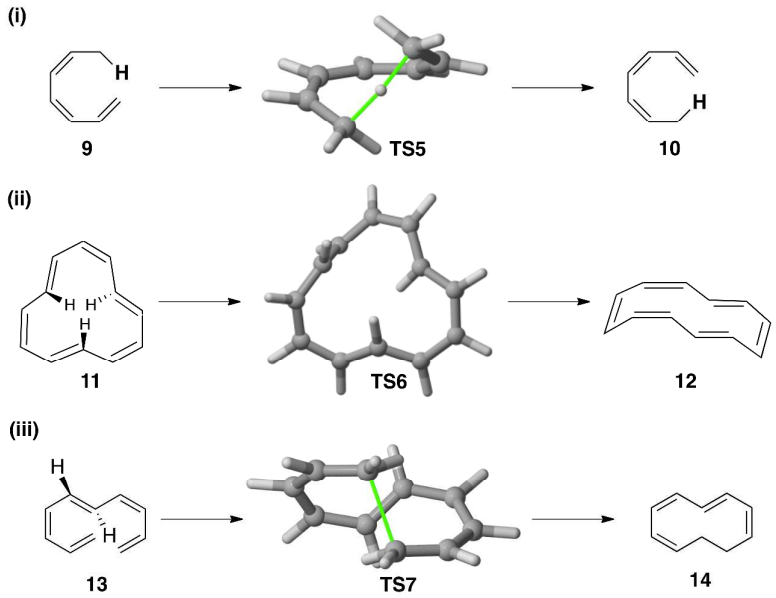

Figure 5. Pericyclic reactions occuring via Möbius aromatic transition structures. (i) [1,7]-sigmatropic hydrogen atom migration in (*Z,Z*)-1,3,5-heptatriene; (ii) isomerization of (*Z*,*E*,*Z*,*E*,*Z*,*E*)-[12]annulene; (iii) electrocyclisation of *Z,E,Z*-decapentaene. Geometries taken from refs. 35a and 38.

The conrotatory electrocyclic ring opening of butadienes is the archetypal thermally allowed pericyclic reaction involving four electrons. "*Torqueselectivity*" was introduced to predict the stereochemistry of their transition structures: electron-donating substituents rotate outwards, whereas electron-withdrawing groups rotate inwards. This concept has been expanded to other systems, e.g., the higher energy electrocyclic ring opening transition states of cyclopropyl anions have less negative NICS values and reduced Möbius aromaticity.[39]

3.1.3. Pericyclic Reactions Involving Transition Metals

This chapter presents examples of recent representative pericyclic reactions involving transition metals that occur through aromatic transition structures.

Fernández, et al.'s DFT computed activation barriers clarified the kinetically controlled regioselectivity for DA reactions between α,β-unsaturated Fischer carbene

complexes **15** with neutral 1,3-dienes, i. e., isoprene and cyclopentadiene, to form 1,4-cycloadducts and *endo*-cycloadducts exclusively (Figure 6).[40a] The transition state geometries of these [4+2] cycloaddition organometallic reactions (analogous to **TS8**) resemble the non-organometallic Lewis-acid complexed α,β-unsaturated esters, and are comparable in synchronicity (S_y = 0.74-0.77 vs. 0.86-0.90) and aromaticity (NICS(0) = –13.5 ppm vs. –17.5 ppm). Likewise, the [3+2] cycloaddition reactions of alkynyl Fischer carbene complexes and nitrones, occur through aromatic transition structures (NICS in the –10.1 to –13.4 ppm range) and are analogous to the isolobal $AlCl_3$-complexed methyl but-2-ynoate.[40b]

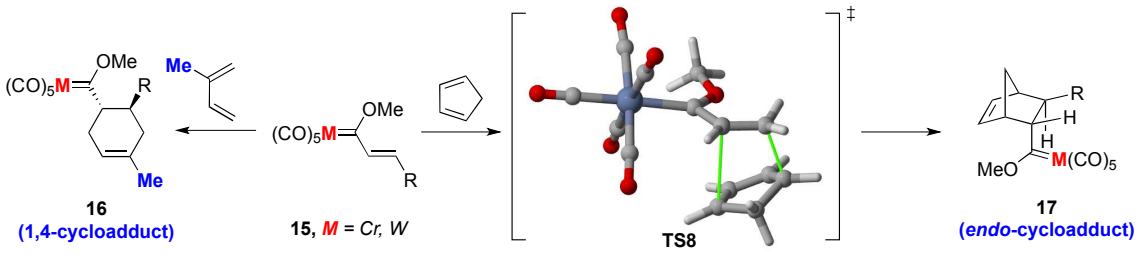

Figure 6. Diels-Alder reactions involving group 6 Fischer alkoxycarbene complexes. Geometry for **TS8** taken from reference 40a.

Alabugin and Krafft's computational and experimental mechanistic study of gold(I)-catalysed propargyl Claisen rearrangement (Figure 7)[41] explained the formation of **18** through the higher energy gold(I)-oxygen complex **17**, rather than **21** through the thermochemically more stable Au-alkyne complex **19**. Reaction through **17** promotes a low barrier cation-accelerated oxonia Claisen pathway (Figure 7) and involves an aromatic transition state (**TS9**, NICS(0) values ca. –15 ppm) akin to uncatalysed Claisen rearrangement transition states (NICS(0) values ca. –18 ppm).

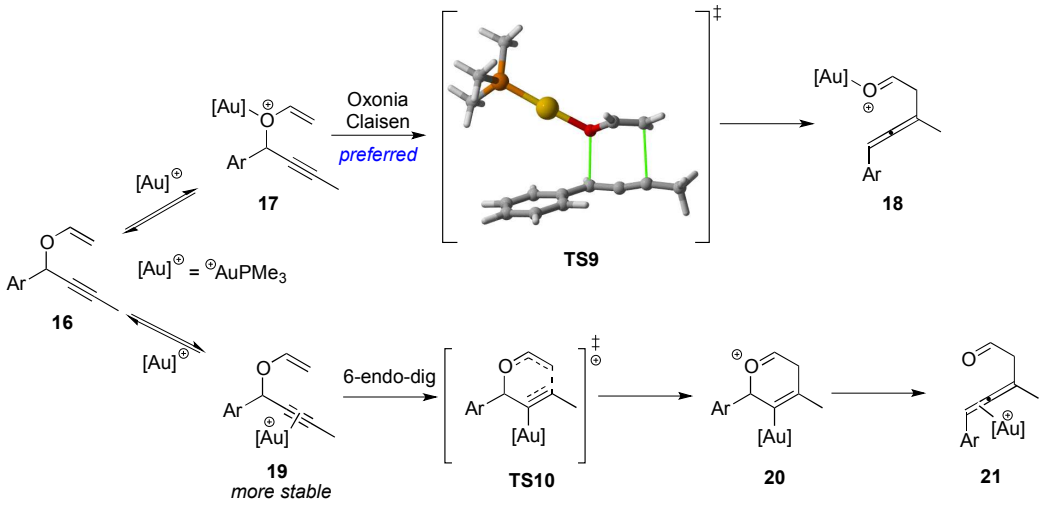

Figure 7. Gold(I)-catalysed Claisen reaction involving propargyl vinyl ethers. Geometry for **TS9** taken from reference 41.

Platinum(II) and gold(I)-catalysed [4+3]-cycloadditions for allene-tethered 1,3-dienes,[42] to form bicyclo[5.3.0]decane skeletons, also involve aromatic transition structures (Figure 8). This transformation proceeds via a concerted organometallic [4+3]-cycloaddition (between the allyl cation and diene moiety), followed by a 1,2-hydrogen shift on the resulting metal-carbene intermediate. The computed ca. −17 ppm NICS(0) value at the (3,+1) ring critical point of **TS11** (see Figure 8) is comparable to the analogous uncatalysed [4+3]-cycloaddition involving a hydroxyoxallyl cation (NICS(0) = −14.4 ppm).

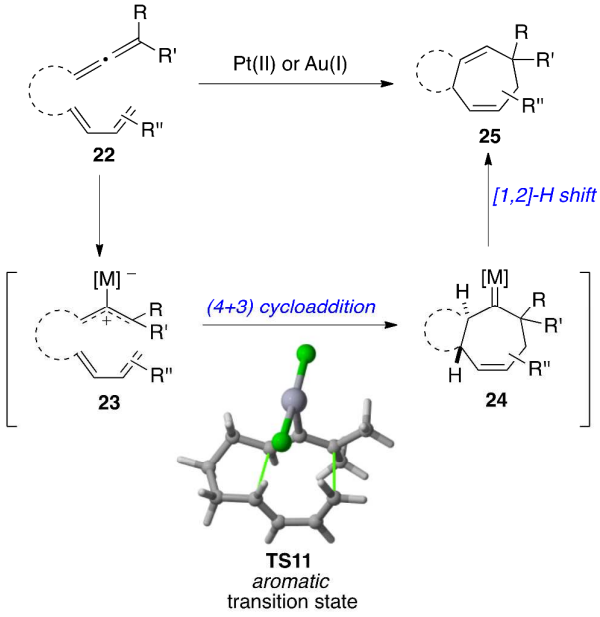

Figure 8. Transition metal catalysed (4+3)-cycloaddition reaction involving an allyl cation. Geometry for **TS11** taken from reference 42.

3.1.4. Double Group Transfer Reactions

Double group transfer (DGT) reactions are a general class of pericyclic reactions involving the simultaneous intermolecular migration of two atoms/groups along a concerted reaction pathway.[43] This definition includes textbook reactions like the diimide reduction of double or triple bonds, the Meerwein-Ponndorf-Verley reduction (MPV) of carbonyl groups, and some type II-dyotropic rearrangements characterized by the intramolecular migration of the two groups (generally hydrogen atoms). Alder-ene reactions also fall into this category as they involve the addition of a multiple bond (enophile) to an alkene (ene) via allylic transposition.

The archetypal DGT reaction is the thermally allowed, concerted, synchronous [$\sigma 2_s + \sigma 2_s + \pi 2_s$] suprafacial transfer of two hydrogen atoms, from ethane to ethylene, which occurs through the highly symmetric planar six-membered ring transition structure **TS12** (Figure 9).[43] Significantly, the equalized CC bond distances have partial double-bond character thereby satisfying the geometric criterion for aromaticity (see Chapter 2). Similar transition structures were computed for related processes involving different types of multiple bonds (alkynes, aldehydes, ketones, or imines).[43]

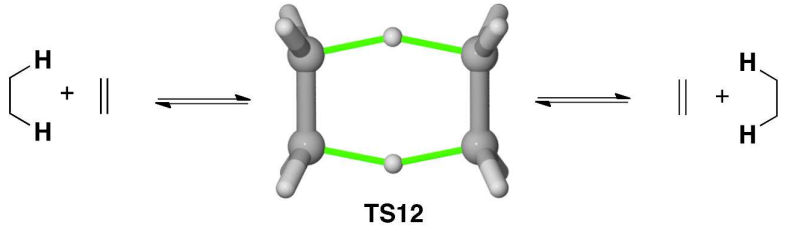

Figure 9. Archetypal DGT reaction between ethane and ethene (see reference 43).

In addition, all these transition structures exhibit sufficiently negative NICS(0) values (in the −10 to −25 ppm range) to fulfil the magnetic criterion for aromaticity: the [$\sigma 2_s+\sigma 2_s+\pi 2_s$]-six electrons involved in the reaction lying at least approximately in the molecular plane give rise to appreciable induced ring currents; these result in a strong diamagnetic shielding at the ring critical point which is responsible for the computed negative NICS values. As shown in Figure 10a, the isotropic NICS grid along the *z* axis (perpendicular to the molecular plane) of **TS12** reveals a bell-shaped curve with a maximum (most negative NICS value) at $z = 0$ Å. The computed ACID plot for **TS12** also sustains a strong diatropic (i.e. aromatic) induced current[23] (Figure 10b). Furthermore, the molecular orbitals of these transition structures closely resemble those for six-membered heteroaromatic rings like pyrazine; hence, such saddle points can be viewed as the in-plane aromatic analogues of heteroaromatic rings.

Despite the aromatic character of these transition structures, DGT reactions are associated with relatively high barriers (typically $\Delta E^{\ddagger} > 40$ kcal/mol). This is due mainly to the energetic penalty required to distort the reactants from their equilibrium geometries to those they must adopt in the corresponding transition structures. This highly destabilizing strain (distortion) energy overcomes the gain in aromaticity during the reaction.[43]

(a) **(b)**

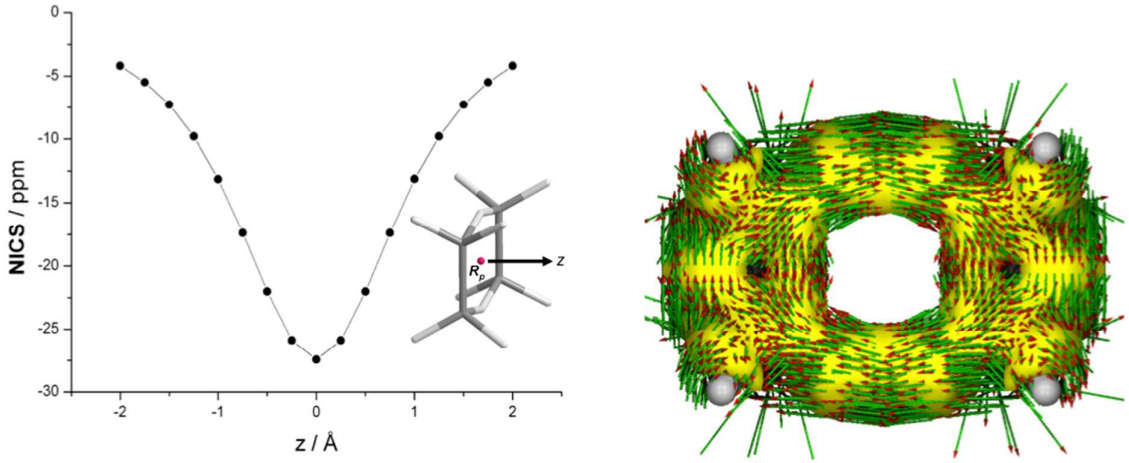

Figure 10. (a) Plot showing the variation of NICS values along the *z* axis perpendicular to the molecular plane. (b) ACID plot of the transition state associated with the ethane + ethene reaction (see reference 43).

Noyori's ruthenium-catalysed hydrogenations of multiple bonds (mainly polar double bonds, i.e. ketones, aldehydes and imines) also involve a double hydrogen atom migration (Figure 11).[44] There is general agreement that the multiple bond reduction occurs in the outer coordination sphere of **A** and therefore does not require any coordinative unsaturation at the transition metal. Therefore, a metal hydride (M–H) intermediate is the reactive species and the hydride delivery to the electrophilic carbon atom takes place via the six-membered pericyclic transition structure **C** (Figure 11). Moreover, the enantioselection of the process is suggested to occur in this crucial pericyclic reaction step.

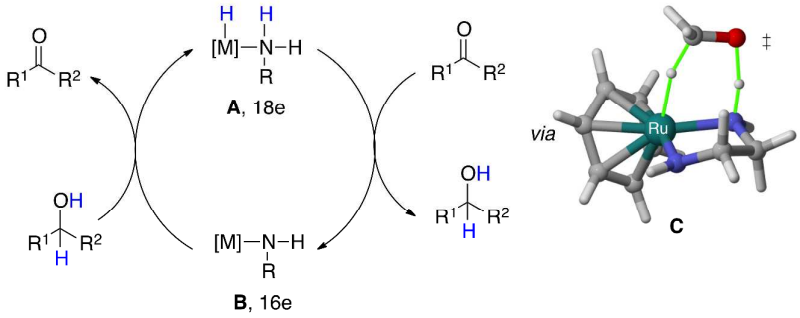

Figure 11. Noyori hydrogenation reaction and associated transition structure. Geometry for transition structure **C** taken from reference 44.

The transition structure associated with the hydrogenation reaction in Figure 11 resembles that described in Figure 9 for the DGT reaction between ethane and ethene. Indeed, the Figure 11 saddle point **C** is in-plane aromatic, in view of its computed equalized bond distances, negative NICS(3,+1) values (from −8.0 to −16.0 ppm, depending on the substrate), and bell-shaped isotropic NICS grids along the *z* axis (cf. Fig. 10a) with a maximum at $z = 0$ (i.e., the (3,+1) ring critical point of the electron density).[44]

3.2. Pseudopericyclic Reactions

In 1976, Lemal et al.[45] reported the unexpected behaviour of perfluorotetramethyl (Dewar thiophene) oxide **26a** (Figure 12). The equivalence of signals observed in the ^{19}F-NMR spectrum even at −95 ºC indicated the existence of a facile degenerate rearrangement with an estimated energy barrier of ca. 6.8 (±0.3) kcal/mol at −100 ºC. Given the bicyclic nature of **26a**, this low-barrier rearrangement should correspond – at least formally – to a thermal [1,3] suprafacial sigmatropic shift, a process forbidden by the Woodward-Hoffman rules. To overcome this mechanistic conundrum, Lemal, et al. proposed the participation of a nonbonding sulphur lone pair in **26a**, implying an alternative nonpericyclic mechanism (Figure 12a).

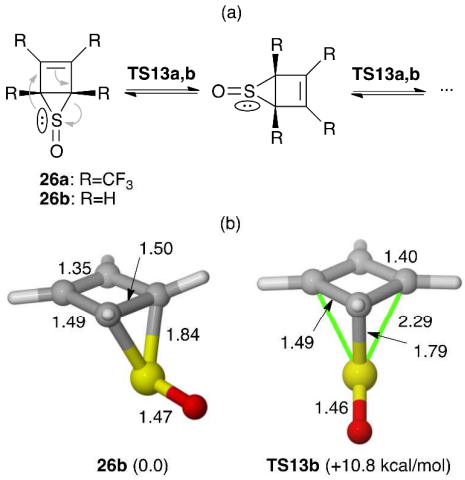

Figure 12. (a) Low energy degenerate thermal rearrangements in Dewar thiophene oxides **26a,b**, according to Lemal. et al. (b) Fully optimized structures of **26b** and **TS13b** (M06-2X/def2-TZVPP level). Distances are given in Å. The relative M06-2X/def2-TZVPP+ΔZPVE energies are in parentheses.

In agreement with Lemal's hypothesis, DFT computations (Figure 12b) reveal a bridged minimum **26b** and nonpericyclic saddle point **TS13b** associated with the degenerate rearrangement of **26b**. The 10.8 kcal/mol activation energy is quite small, considering the lower electrophilicity of the alkene moiety of **26b** with respect to that expected for **26a**.

This novel rearrangement, apparently corresponding to a symmetry-forbidden process, led Lemal to identify a general kind of reactions for which he coined the term *pseudopericyclic*. According to this proposal, "*a pseudopericyclic reaction is a concerted transformation whose primary changes in bonding compass a cyclic array of atoms, at one (or more) of which nonbonding and bonding atomic orbitals interchange roles*".[45] This in turn implies two disconnections in the cyclic array of the overlapping orbitals (in sharp contrast with Hückel or Möbius aromatic pericyclic reactions, vide supra) because the atomic orbitals that interchange roles lie in orthogonal planes (Figure 13). Birney et al.[46] studied such reactions extensively and concluded that they are always symmetry-allowed, regardless of the

number of electrons involved. Also as a consequence of their special features, such reactions take place with very low or negligible activation barriers via nearly planar transition structures (with obvious exceptions such as **TS13** in Figure 12b) and are favoured when optimal electrophilicity-nucleophilicity matching occurs. Following these criteria, many well-known chemical reactions can be described as pseudopericyclic. For instance, Birney et al. have shown that thermal *syn* β−eliminations can be considered as pseudopericyclic reactions.

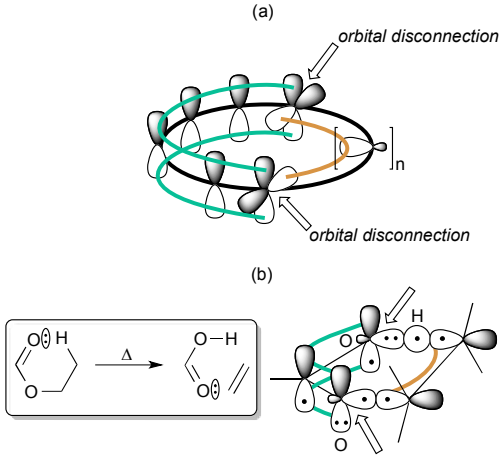

Figure 13. (a) Schematic general representation of orbital disconnections (highlighted as hollow arrows) in a pseudopericyclic reaction, with n=0,1,2,... (b) Atomic orbital representation of a thermal *syn* β−elimination, according to Birney et al. (see ref. 46).

Following Lemal's lead, many transformations have been identified as being pseudopericyclic. For example, pseudopericyclic prototropic and silatropic[47] [1,*n*] shifts as well as [3,5] shifts[48] shown in Figure 14 involve switching functions between s-, p- and nonbonding atomic orbitals.

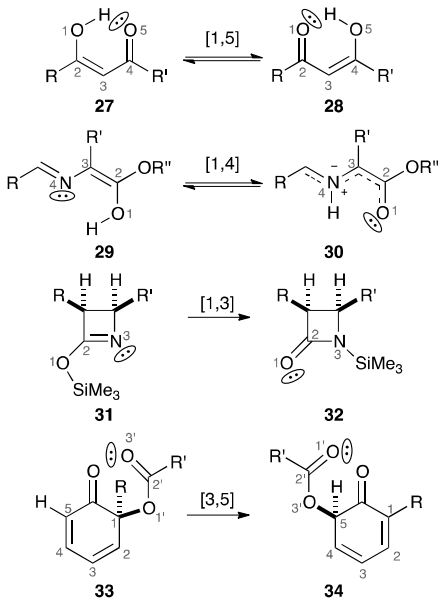

Figure 14. Selected examples of pseudopericyclic sigmatropic shifts.

There also are examples of pseudopericyclic additions and cycloadditions like those given in Figure 15.[46] Note that nonbonding atomic orbitals of reactants/products in pseudopericyclic reactions can be empty, as in the hydroboration of alkenes, a process identified by Lemal as being pseudopericyclic. The selected examples of pseudochelotropic and pseudo-electrocyclic reactions, also included in Figure 15, confirm the ubiquity of pseudopericyclic reactions in chemistry.

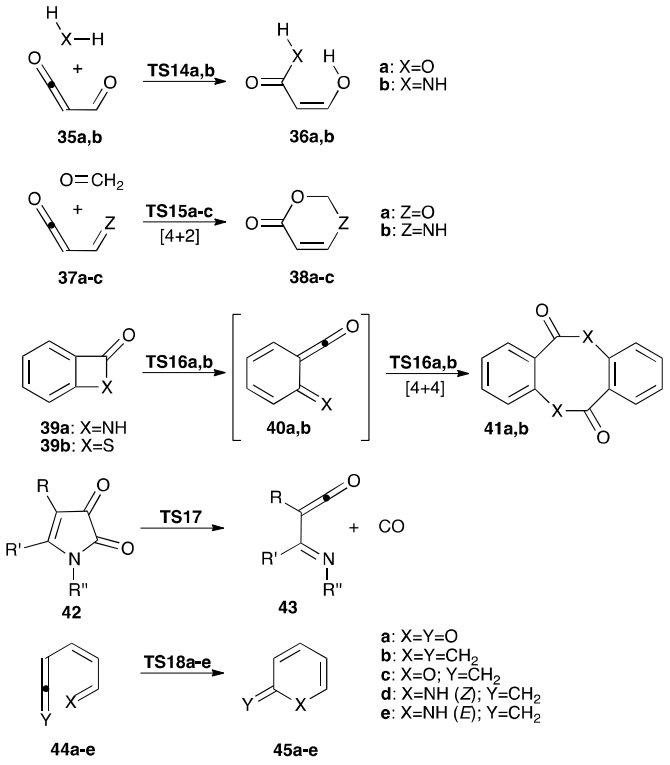

Figure 15. Selected examples of pseudopericyclic and pseudocycloadditions as well as pseudochelotropic and pseudoelectrocyclic reactions (with the exception of the **44b** → **45b** transformation).

While some borderline cases are controversial, pseudopericyclic and pericyclic reactions are most effectively distinguished by the near planar transition structure and lower activation energy of the former.[49] A comparison of the pericyclic **44b**→**45b** reaction (via the aromatic **TS18b**) and pseudopericyclic **44e**→**45e** reaction (via the nonaromatic **TS18e**) is instructive. As shown in Figure 16, the less planar **TS18b** displays a larger ω dihedral angle than **TS18e**. Accordingly, the computed isotropic NICS at the ring critical point of **TS18b** (–13.6 ppm) is twice as negative compared to **TS18e** (–5.6 ppm) (Figure 16). ACID plots of both saddle points show a closed circuit in **TS18b** together with a diamagnetic ring current, whereas **TS18e** displays a breached ring current, as expected by the orbital disconnections associated with a pseudopericyclic process. MO and CASSCF analyses, the Laplacian of electron density, electron fluctuation, the electron localization function (ELF), and the

ellipticity of the electron density are among other useful criteria for distinguishing pseudopericyclic and pericyclic reactions.

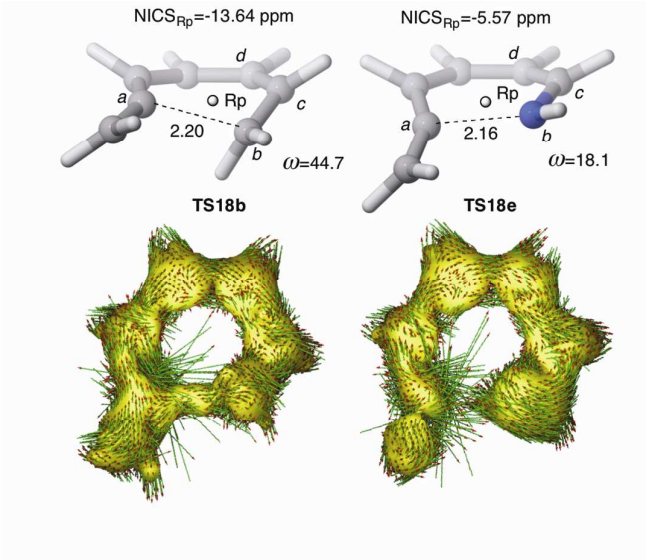

Figure 16. Main geometric and magnetic features of fully optimized transition structures **TS18b** and **TS18e** (at the M06-2X/def2-TZVPP level). Bond distances and angles are given in Å and deg., respectively. Dihedral angles (in absolute values) ω are defined as ω=*a-b-c-d*. The NICS values at the ring points of electron density (Rp) and the ACID plots are also reported.

3.3. Nonpericyclic Reactions

Aromatic transition structures also can facilitate nonpericyclic transformations. However, distinctions between cyclic non-aromatic transition structures and their corresponding pericyclic analogues are not always straightforward. For instance, Dewar and Mertz interpreted the cyclic Zimmerman-Traxler-like transition state geometry computed for the Reformatsky reaction[50] as "a [3,3]-sigmatropic shift, analogous to a Cope or Claisen rearrangement".

Other nonpericyclic reactions involving aromatic transition structures have been reported. Based on computed dissected NICS, Alabugin, et al. noted that the five-membered ring 5-*endo*-dig and 5-*endo*-trig anionic ring closure transition structures (see Figure 17) are in-plane aromatic.[51] These nonpericyclic transformations involve the in-plane delocalization

of six electrons, i. e., a lone pair, σ-CC bond, and the in-plane alkyne, or alkene, π-bond (see Figure 17, participating bonds/lone pair in red). Replacement of the anionic CH_2^- centre by an isoelectronic NH^- or O^- group reduces the transition state aromaticity, as the higher electronegativity of N and O restricts effective σ electron delocalization of the lone pair.

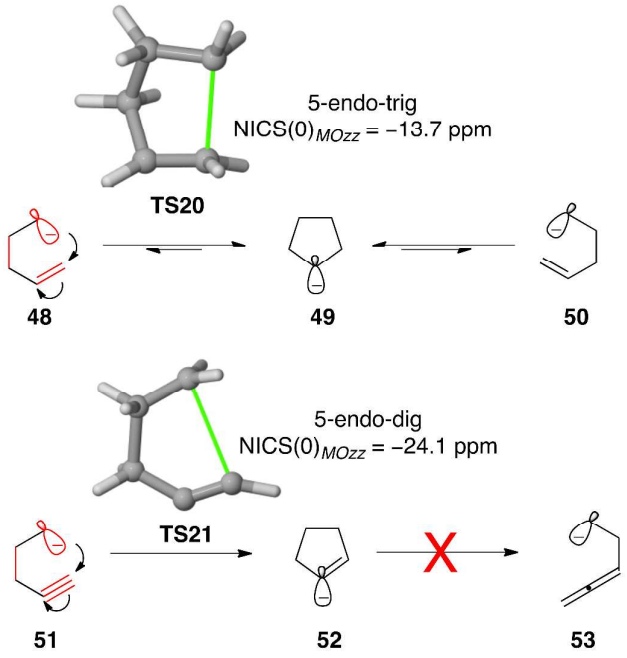

Figure 17. [5-*endo*-*trig*] and **[**5-*endo*-*dig*] processes studied by Alabugin and co-workers (see reference 51).

Alabugin et al., coined the term "aborted" anionic [2,3]-sigmatropic shifts for these nonpericyclic anionic cyclizations. The participating σ-CC bond is elongated but not broken, thus affording additional thermochemical stabilization for the cyclic minimum (see **49** and **52** in Figure 17). Such reactions differ from "concerted" processes, characterized by a transition structure between the degenerate reactant and product, and from "interrupted" processes, in which one or more intermediates exist and are higher in energy than the reactant/product. "Aborted" anionic [2,3]-sigmatropic shifts, e.g., the 5-*endo*-*dig* reaction in Figure 17, form low energy products (e.g., **52**) that preclude further reaction (e.g., to form **53**). Competition among concerted, interrupted, and aborted sigmatropic shifts can be controlled electronically

by selectively stabilizing various positions of the intervening cyclic transition structures or intermediates.[51]

4. Concluding Remarks and Outlook

This Tutorial review summarizes current computational methods for identifying aromatic transition structures, and illustrates representative examples of pericyclic, pseudo-pericyclic and non-pericyclic reactions involving aromaticity and non-aromaticity. The tremendous development of Computational Chemistry during the past decades provide chemists with a robust theoretical framework and very helpful tools to generalize the concept of aromaticity and its application to transition structures (which are not accessible for direct experimental study). The computation-based discovery that aromatic transition states can participate in non-pericyclic reactions (Section 3.3),[51] exemplifies the effectiveness of theoretical approaches for recognizing novel chemical transformations. Despite caveats that aromaticity is just a chemical bonding model without a quantifiable, precise meaning,[2] it remains a highly popular and essential concept in chemistry accounting for anomalous properties such as geometry, reactivity and magnetic behaviour. Aromatic transition structures extend the applicability of *aromaticity* to "closed circuit" structures generally.

Acknowledgments. This work was supported by the USA NSF Grant CHE-105-7466 and by the Spanish Spanish Secretaría de Estado de Investigación, Desarrollo e Innovación and CAM (Grants CTQ2010-20714-C02-01, CTQ2010-16959, Consolider-Ingenio 2010, CSD2007-00006, S2009/PPQ-1634).

References and Notes

[1] M. G. Evans and E. Warhurst, *Trans. Faraday Soc.*, 1938, **34**, 614.
[2] G. Frenking, A. Krapp, *J. Comput. Chem*. 2007, **28**, 15.
[3] H. Jiao and P. v. R. Schleyer, *J. Phys. Org. Chem.*, 1998, **11**, 655, and references therein.
[4] M. G. Evans, *Trans. Faraday Soc.*, 1939, **35**, 824.
[5] R. B. Woodward and R. Hoffmann: *The Conservation of Orbital Symmetry*; Verlag Chemie, Weinheim, 1970.
[6] (a) H. Zimmerman, *Acc. Chem. Res*. 1971, **33**, 272; (b) M. J. S. Dewar, *Angew. Chem. Int. Ed. Engl*., 1971, **10**, 761.
[7] Z. Chen, C. S. Wannere, C. Corminboeuf, R. Putcha and P. v. R. Schleyer, *Chem. Rev.* 2005, **105**, 3842.
[8] I. Fernández and G. Frenking, *Faraday Discuss*. 2007, **135**, 403, and references therein.
[9] W. v. E. Doering, W. R. Roth, R. Breuckman, L. Figge, H.-W. Lenartz, W. D. Fessner and H. Prinzbach, *Chem. Ber.*, 1988, **121**, 1.
[10] P. v. R. Schleyer, M. Manoharan, H. Jiao and F. Stahl, *Org. Lett.* 2001, **3**, 3643.
[11] P. Bultinck, *Faraday Discuss.*, 2007, **135**, 347, and references therein.
[12] (a) R. Gleiter and G. Haberhauer: *Aromaticity and Other Conjugation Effects*; Wiley-VCH: Weinheim, **2012**; pp 28-46 and references therein. Equalized bond lengths in benzene arise from sigma rather than pi electron delocalization; for recent explanations, see: (b) S. C. A. H. Pierrefixe and F. M. Bickelhaupt, *Chem. Eur. J.*, 2007, **13**, 6321 and reference 8.
[13] A. de Cózar and F. P. Cossío, *Phys. Chem. Chem. Phys*. 2011, **13**, 10858, and references therein.
[14] S. Sakai, *J. Phys. Chem. A* 2006, **110**, 6339, and references therein.
[15] L. Pauling, *J. Chem. Phys.*, 1936, **4**, 673.
[16] F. London, *J. Phys. Radium*, 1937, **8**, 397.
[17] J. A. Pople, *J. Chem Phys.*, 1956, **24**, 1111.
[18] H. J. Dauben Jr., J. D. Wilson and J. L. Laity, *J. Am. Chem. Soc.*, 1968, **90**, 811.
[19] P. v. R. Schleyer, C. Maerker, A. Dransfeld, H. Jiao and N. J. r. V. E, Hommes, *J. Am. Chem. Soc.*, 1996, **118**, 6317.
[20] H. Fallah-Bagher-Shaidaei, C. S. Wannere, C. Corminboeuf, R. Puchta and P. v. R. Schleyer, *Org. Lett.*, 2006, **8**, 863 and references therein.
[21] C. Corminboeuf, T. Hein, G. Seifert and P. v. R. Schleyer, *J. Phys. Chem. Chem. Phys*., 2004, **6**, 273.
[22] H. Fliegl, S. Taubert, O. Lehntonen and D. Sundholm, *Phys. Chem. Chem. Phys*. 2011, **13**, 20500, and references therein.
[23] D. Geuenich, K. Hess, F. Köhler and R. Herges, *Chem. Rev.*, 2005, **105**, 3758, and references therein.
[24] W. V. E. Doering and G. H. Beasley, *Tetrahedron*, 1973, **29**, 2231, and references therein.
[25] B. Beno, K. N. Houk and D. A. Singleton, *J. Am. Chem. Soc.*, 1996, **118**, 9984, and references therein.
[26] R. V. Williams, *Chem. Rev*. 2001, **101**, 1185, and references therein.
[27] F. P. Cossío, I. Morao, H. Jiao and P. v. R. Schleyer, *J. Am. Chem.Soc.* 1999, **121**, 6737.
[28] See, for instance, R. D. Bach, G. J. Wolber and H. B. Schlegel. *J. Am. Chem. Soc.*, 1985, **107**, 2837.
[29] S. S. Shaik and P. C. Hiberty: *A Chemist's Guide to Valence Bond Theory*; Wiley: Hoboken, 2008; pp 185-186.
[30] K. N. Houk, *Acc. Chem. Res.* 1975, **8**, 361.
[31] J. W. McIver, *Acc. Chem. Res.* 1974, **7**, 73.
[32] H. S. Rzepa and W. A. Wyle, *J. Chem. Soc. Perkin Trans. 2* **1991**, 939.
[33] R. W. Alder, J. N. Harvey, G. C. Lloyd-Jones and J. M. Oliva, *J. Am. Chem. Soc.* 2010, **132**, 8325.
[34] A. Arrieta, M. C. de la Torre, A. de Cózar, M. A. Sierra, *Synlett* 2013, **24**, 0535 and references therein.

[35] For an excellent review on Möbius aromaticity, see: (a) H. S. Rzepa, *Chem. Rev*. 2005, **105**, 3697. See also, (b) W. C. McKee, J. I. Wu, H. S. Rzepa and P. v. R. Schleyer, *Org. Lett.* 2013*,* **15**, 3432.
[36] E. Heilbronner, *Tetrahedron Lett*. 1964, **5**, 1923.
[37] M. Mauksch, V. Gogonea, H. Jiao and P. v. R. Schleyer, *Angew. Chem. Int. Ed*., 1998, **37**, 2395.
[38] H. S. Rzepa, *Chem. Comm*. 2005, 5220.
[39] O. Nieto-Faza, C. Silva-López, A. B. González-Pérez, M. Pérez-Rodríguez and A. Rodríguez de Lera, *J. Phys. Org. Chem.,* 2009, **22**, 378 and references therein.
[40] (a) I. Fernández, M. A. Sierra and F. P. Cossío, *J. Org. Chem*. 2008, **73**, 2083; (b) I. Fernández, M. A. Sierra and F. P. Cossío, *J. Org. Chem*. 2006, **71**, 6178.
[41] D. V. Vidhani, J. W. Cran, M. E. Krafft, and I. V. Alabugin, *Org. Biomol. Chem*., 2013, **11**, 1624.
[42] I. Fernández, F. P. Cossío, A. de Cózar, A. Lledós and J. L. Mascareñas, *Chem. Eur. J*., 2010, **16**, 12147.
[43] I. Fernández, F. M. Bickelhaupt, and F. P. Cossío, *Chem. Eur. J*., 2009, **15**, 13022 and references therein.
[44] O. Nieto Faza, C. Silva López and I. Fernández, *J. Org. Chem*., 2013, **78**, 5669, and references therein.
[45] J. A. Ross, R. P. Seiders, D. M. Lemal, *J. Am. Chem. Soc.,* 1976, **98**, 4325.
[46] D. M. Birney, *Curr. Org. Chem*., 2010, **14**, 1658, and references therein.
[47] A. Arrieta, F. P. Cossío and B. Lecea, *J. Org. Chem.,* 2000, **65**, 8458.
[48] S. Sharma, T. Rajale, D. B. Cordes, F. Hung-Low and D. M. Birney, *J. Am. Chem. Soc.,* 2013, **135**, 14438.
[49] S. M. Bachrach, *Computational Organic Chemistry*, Wiley-Interscience: Hoboken, NJ, pp 170-177 and references therein.
[50] M. J. S. Dewar and K. M. Mertz, *J. Am. Chem. Soc.,* 1987, **109**, 6553.
[51] K. Gilmore, M. Manoharan, J. I-C. Wu, P. v. R. Schleyer and I. V. Alabugin, *J. Am. Chem. Soc*., 2012, **134**, 10584.

Paul von Ragué Schleyer was born in Cleveland, Ohio. After education at Princeton and Harvard (Ph.D. in physical organic chemistry with P. D. Bartlett), he returned to Princeton as Instructor in 1954 and was named Eugene Higgins Professor of Chemistry in 1969. Needing more computer time, he accepted in 1976 the Chair once held by Emil Fischer and became Co-Director of the Organic Institute of the University of Erlangen-Nuremberg, Germany. He founded its Computer Chemistry Center in 1993. Schleyer has been Professor Emeritus at Erlangen since 1998, and continues as Graham Perdue Professor of Chemistry at the University of Georgia, Athens. He is past President of the World Association of Theoretically-Oriented Chemists (WATOC), a Fellow of the Bavarian Academy, the International Academy of Quantum Chemical Science, and the American Academy of Arts and Sciences, and was the Editor-in-Chief of the Encyclopedia of Computational Chemistry.

Judy I-Chia Wu (Taiwan, 1982) earned her Ph.D. with Paul von Ragué Schleyer at the Center for Computational Quantum Chemistry, University of Georgia (UGA) in 2011. She is one of the recipients of the 2012 IUPAC Young Chemist Prize, and is currently an Assistant Research Scientist at UGA. Her research interest in developing chemical concepts through applications of Computational Chemistry contributes to understanding aromaticity, hyperconjugation, strain in molecules, and reexamines physical organic interpretations from a modern viewpoint.

Fernando P. Cossío studied chemistry at the Universidad de Zaragoza (Spain) and received his PhD in 1986 at the University of the Basque Country (UPV/EHU, Spain, Prof. C. Palomo). After a postdoctoral stay at CNRS (Talence, France, Dr J.-P. Picard), he joined the UPV/EHU as *Profesor Titular* in 1988 and *Catedrático* in 2002. In 1994, after a short stay at UCLA in the laboratories of Prof. K. N. Houk, he decided to combine theoretical and experimental organic chemistry to investigate the origins of selectivity in chemical reactions. His research interests include pericyclic reactions, C–C bond-forming reactions, and medicinal chemistry (design and chemical synthesis of inhibitors of integrins and epigenetic enzymes). At present, F.P.C. is the Scientific Director of Ikerbasque, The Basque foundation for science.

Israel Fernández (Madrid, 1977) studied Chemistry at the Universidad Complutense of Madrid (UCM). In 2005, he earned his Ph.D. (with honors) at the UCM under the supervision of Prof. Miguel A. Sierra receiving the Lilly-Young Researcher Award. After that, he joined the Theoretical and Computational Chemistry group of Prof. Gernot Frenking at the Philipps Universität Marburg as a postdoctoral researcher. In 2009, he received the Young-Researcher Award from the Spanish Royal Society of Chemistry and the Julián Sanz del Río award in 2011. At present, I.F. is *Profesor Contratado Doctor* at the UCM. His current research includes the experimental and computational study of the bonding situations and reaction mechanisms of organic and organometallic compounds.